F

FRACTURE BEHAVIOUR AND TENSILE PROPERTIES OF TITANIUM ALLOYS AT ELEVATED TEMPERATURES

A. Gysler* and G. Lütjering**

INTRODUCTION

The application of commercial titanium alloys at elevated temperatures is limited to the region below about 773 K. Compared to other materials with similar high melting points, e.g. nickel-base alloys, titanium alloys cannot be considered as outstanding high temperature alloys. It is still uncertain which microstructural features are responsible for the sharp drop of the yield stress occurring in titanium alloys in the temperature region above about 723 K [1].

With regard to tensile deformation at room temperature high strength alloys often show three different types of fracture modes, depending on the microstructure, as shown in Figure 1 [2]. If the alloy forms intense slip bands the cracks propagate along these slip bands (A). If the microstructure exhibits soft, precipitate free zones (PFZ) along grain boundaries which deform preferentially, the cracks propagate within these zones (B). If the alloy contains incoherent particles voids are formed at these particles during plastic deformation and fracture occurs by void coalescence (C). The objective of the present study was to investigate the short time tensile properties and the fracture behaviour at elevated temperatures of a variety of well-defined model structures in binary titanium alloys. Ti-Mo alloys were chosen because the deformation behaviour and the fracture characteristics at room temperature are already known [3,4].

EXPERIMENTAL PROCEDURE

The experiments were performed on two Ti-Mo alloys with 8.7 and 14.1 at % molybdenum. The oxygen content was about 3000 ppm for both alloys. Tensile specimens with diameters of 5 mm and gauge lengths of 25 mm were machined from rods which were prior hot worked in the β-phase field (Ti-8Mo) or cold deformed at room temperature (Ti-14Mo). All specimens were solution treated in the β-phase field at 1273 K for 1h in vacuum ($< 10^{-4}$ Pa) and quenched to room temperature. In addition the Ti-14Mo alloy was tested with two different grain sizes of 30 µm (1h 1073 K) and 180 µm (1h 1273 K/1h 1073 K). By varying the aging temperature and time a variety of different microstructures could be obtained [5]. The resulting microstructural parameters are summarized in Table 1. Both of the alloys exhibit in the underaged condition, Ti-8Mo annealed for 10h at 723 K and Ti-14Mo for 100h at 623 K (Table 1), a typical microstructure for fracture mode A [3]. The Ti-14Mo alloy in the aging condition 100h 723 K contains, in addition to the ω-particles within the matrix, narrow precipitate free zones (width about 30 nm) along grain boundaries resul-

*DFVLR, Cologne, Germany.
**Ruhr-University, Bochum, Germany.

ting from vacancy depletion [5]. In the present work a fine distribution of small α-particles (size about 5-10 nm) could be detected within the grain boundaries indicating that also solute depletion contributes to the appearance of the PFZ. This alloy condition exhibits fracture mode B at room temperature [4]. Step aging of Ti-8Mo leads to needle like α-particles within the matrix and to the precipitation of somewhat larger α-particles along grain boundaries [6]. This alloy showed predominantely fracture mode C if tested at room temperature. The tensile tests, with a strain rate of 6.7×10^{-4} sec^{-1}, were performed in air in the region between room temperature and the aging temperature of the corresponding microstructure as an upper limit. The fracture surfaces and in a few cases the electrolytically polished surface of deformed specimens were investigated by scanning electron microscopy.

EXPERIMENTAL RESULTS

The description of the results can be divided conveniently into three sections, following the three basic fracture mechanisms at room temperature schematically outlined in Figure 1.

Fracture Mode A

The tensile properties ($\sigma_{0.1}$, σ_f, ε_f) of the two alloys in the underaged condition are shown in Figure 2 as a function of deformation temperature. It can be seen that both, the yield stress and the true fracture stress decreased with increasing test temperature. The striking feature in Figure 2 is the drastic difference in the temperature dependence of the yield stress for both alloys. The alloy with a high volume fraction of coherent ω-particles (Table 1) exhibits only a weak temperature dependence of the yield stress, declining about 200 MPa over the whole temperature range investigated. In contrast, the alloy with a much lower particle volume fraction shows in the narrow range between room temperature and 523 K a drastic drop of the yield stress (300 MPa).

The ductility ε_f of the alloy with a high volume fraction of particles is almost zero up to test temperatures of about 523 K and starts to rise only gradually up to a maximum value of 0.1 at 723 K (Figure 2). On the other side the fracture strain at room temperature of the Ti-14Mo alloy in the underaged condition is quite high, showing a value of more than 0.7. With increasing test temperature the ductility increases for this alloy to almost 0.9 as the yield stress drops to lower values.

The fracture surface investigations showed that at room temperature deformation of the Ti-8Mo alloy with the high yield stress and the low ductility, fracture occurred mainly along slip bands as may be seen from Figure 3a in agreement with the proposed model schematically drawn in Figure 1(A). With rising test temperature up to 723 K the fracture changed to a predominantly dimple type of fracture mode along grain boundaries (Figure 3b). This transition occurred gradually in the intermediate temperature region. By aging the Ti-14Mo alloy at 623 K the volume fraction of ω-particles within the matrix was reduced to such an extent that crack propagation at room temperature deformation occurred no longer along slip bands: A mixed topography was found with grain boundary fracture as well as a dimple type of fracture mode caused by void nucleation and coalescence (Figure 3c). With increasing test temperature the portions of matrix failure by dimple rupture predominate over grain boundary fracture as can be seen in Figure 3d.

Fracture Mode B

The Ti-14Mo alloy aged 100h at 723 K (condition B) was investigated with two different grain sizes of 30 μm and 180 μm (Table 1). The corresponding tensile properties as a function of deformation temperature are shown in Figure 4. It can be seen that the yield stress and the true fracture stress decreased with increasing temperature for both grain sizes. Within experimental error, no difference in the absolute values of the yield stresses and therefore in the temperature dependence was found for the two different grain sizes, as shown in Figure 4. The slope of the yield stress versus temperature curve and the absolute values are almost comparable with the corresponding curve for the Ti-14Mo alloy in the underaged condition in Figure 2.

In contrast to the coinciding yield stress curves the temperature dependence of the ductility differed completely for specimens with the two different grain sizes. Specimens with the large grain size exhibited true fracture strains ε_f below 0.1 up to about 373 K, the ductility is then rising conspicuously within a relatively narrow temperature region between 373 K and 473 K to values of more than 0.7, as may be seen in Figure 4. On the other side the ductility of specimens with a small grain size is quite high at room temperature showing values of about 0.7 [4]. Again above about 373 K the curve starts to increase reaching values of almost 1.2 at a deformation temperature of 723 K.

Surface observations of electrolytically polished and deformed specimens showed that grain boundary sliding occurred in condition B of this alloy [4]. It was found that this process takes place in specimens of both grain sizes and at all deformation temperatures investigated. Examples are shown in the scanning electron micrographs in Figure 5, where the sliding of adjacent grains against each other is demonstrated by the shearing of small markers, scratched on the specimen surface parallel to the tensile axis before deformation.

The fracture surface examination of the Ti-14Mo alloy in condition B showed that grain boundary fracture occurred in specimens of both grain sizes if tested at room temperature, as can be seen from Figures 6a and c. With increasing test temperature the fracture topography of specimens with the small grain size changed from the intercrystalline fracture to a transcrystalline fracture caused by void coalescence. This is shown in Figure 6b, where large dimples can be observed with distances of about 50 μm. On the other side the fracture surfaces of specimens with the large grain size showed an intercrystalline fracture behaviour over the whole range of deformation temperatures investigated. Due to the high true fracture strains at test temperatures above 473 K the grains are elongated extensively in the direction of tensile loading as can be seen from the fracture surface (Figure 6d).

Fracture Mode C

The tensile properties of the Ti-8Mo alloy are shown in Figure 7. It can be seen that the yield stress and the fracture stress decrease continuously with increasing test temperature. Compared to the other stress versus temperature curves (Figures 2 and 4) the fracture stress decreased more rapidly, declining from over 1200 MPa to less than 800 MPa as the deformation temperature was raised from room temperature to 773 K.

The temperature dependence of the fracture strain ε_f also differed from the curves found for all of the other microstructures. It can be seen

from Figure 7 that the ductility showed only a weak temperature dependence with a flat maximum between about 423 K and 573 K. At higher test temperatures the ductility decreased from 0.15 to about 0.06 at 773 K as shown in Figure 7.

The corresponding fracture surfaces in Figure 8 make clear that a transition occurred from a predominantly transcrystalline fracture mode at room temperature (Figure 8a) to an intercrystalline fracture behaviour which dominates at 773 K (Figure 8b). The dimples on the relatively flat portions in Figure 8a and on the less frequently observable sites in Figure 8b where transcrystalline fracture occurred, had average spacings of 8 µm as can be seen in Figure 8c. The flat dimples covering the grain boundaries in Figures 8a and b were much smaller with spacings of about 2 µm (Figure 8d).

DISCUSSION

By varying the microstructure of the titanium alloys investigated the tensile properties and the fracture behaviour as a function of test temperature varied within broad limits (Figures 2, 4 and 7). Besides phase stability and acceptable creep properties, the objectives of developing microstructures for application at elevated temperatures have to be a high yield stress over the whole range of service temperatures and a high ductility, again with a weak temperature dependence. Without considering the creep properties the following conclusions can be drawn from the experimental results of this study. From the point of view of a high yield stress over the whole range of temperatures an alloy with a high volume fraction of coherent particles would be desirable (Figure 2, Ti-8Mo). The densely packed particles prevent extensive cross slip processes of screw dislocations in order to avoid the particles. The yield stress, therefore shows only a weak temperature dependence (Figure 2), approximately following the temperature dependence of the elastic constants [7]. However, the high volume fraction of particles results in an extremely brittle behaviour at lower test temperatures due to large dislocation pile-ups against grain boundaries, causing grain boundary shearing and fracturing [3]. Lowering the volume fraction of coherent particles within the matrix leads to the desirable high ductility over the whole range of temperatures (Figure 2, Ti-14Mo), due to the decreasing number of dislocations within the pile-ups as a result of the lower particle hardening value. As shown in Figure 2 this can be achieved only at the expense of the high yield stress. Furthermore the low particle volume fraction facilitates cross slip processes of dislocations with increasing temperature. Such a transition seems to be responsible for the drastic drop of the yield stress within a narrow range of temperature (Figure 2). It should be emphasized that another possibility of increasing the ductility at room temperature for this fracture mode A is a reduction in grain size [8]. The high temperature properties of this structure are under investigation.

The temperature dependence of the yield stress for condition B of Ti-14Mo (Figure 4) is similar to the underaged condition of this alloy (Figure 2) because for both conditions the volume fraction of ω-particles is low. The detrimental influence of precipitation free zones along grain boundaries on the ductility at lower temperature (Figure 4, large grain size), can be compensated by reducing the grain size of the alloy (Figure 4, small grain size). The reduced length of each grain boundary deforming preferentially prevents early crack nucleation at grain boundary triple points [4]. This beneficial effect together with the diminishing difference between the yield stress of matrix and PFZ with increasing test temperature gives rise to an almost homogeneous deformation behaviour. Void nucleation at hard inclusions, always present in these alloys [3] and void coalescence are now determining the fracture behaviour, as can be seen from the dimple type of fracture mode visible in Figure 6b.

A high volume fraction of particles per se cannot be considered as a criterion for high yield stress values at elevated temperatures as can be seen from Figure 7. If these particles are incoherent with the matrix, as in the case of the β + α structure under investigation, the yield stress decreases more rapidly than one would expect from the temperature dependence of the elastic constants. The reason for this behaviour is subject to further investigations, especially with regard to commercial α + β alloys. The observed decrease of the ductility at higher test temperatures of the β + α microstructure (Figure 7) can also be observed in commercial α + β titanium alloys [1]. The possible reason for this behaviour is thought to be related to the decohesion of the β/α interface with increasing test temperature.

An evaluation of all of the different microstructural parameters with regard to an improvement of short time tensile properties at elevated temperatures results in the combination of a high volume fraction of coherent particles and a small grain size.

REFERENCES

1. CHANG, J. C., The Science, Technology and Application of Titanium, eds. R. I. Jaffee and N. E. Promisel, Pergamon Press, N.Y., 1970, 1053.
2. LÜTJERING, G., ESA TT-245, 1976.
3. GYSLER, A., LÜTJERING, G. and GEROLD, V., Acta Met., 22, 1974, 901.
4. PETERS, M. and LÜTJERING, G., Z. Metallkde., 67, 1976, 811.
5. GYSLER, A., BUNK, W. and GEROLD, V., Z. Metallkde., 65, 1974, 411.
6. WILLIAMS, J. C., Titanium Science and Technology, eds. R. I. Jaffee and H. M. Burte, Plenum Press, N.Y., 1973, 1433.
7. CONRAD, H., DONER, M. and DE MEESTER, B., Titanium Science and Technology, eds. R. I. Jaffee and H. M. Burte, Plenum Press, N.Y., 1973, 969.
8. GYSLER, A., TERLINDE, G. and LÜTJERING, G., Proc. 3rd Int. Conf. on Titanium, Moscow, 1976.

Table 1 Alloy Conditions and Microstructural Parameters

Fracture Mode	Alloy	Aging	Structure	Particle Size	Volume Fraction	Grain Size
A	Ti-8Mo	10h 450°C	β + ω	25 nm	high	250 µm
	Ti-14Mo	100h 350°C	β + ω	6 nm	low	180 µm
B	Ti-14Mo	100h 450°C	β + ω +PFZ	10 nm	low	30 µm 180 µm
C	Ti-8Mo	48h 450°C +24h 500°C	β + α	250 nm	high	250 µm

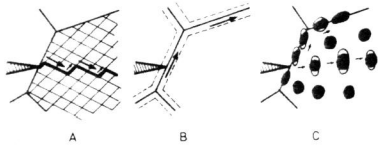

Figure 1 Fracture Mechanisms at Room Temperature (Schematically)
A) Slip Band Fracture
B) Grain Boundary Fracture (PFZ)
C) Void Coalescence

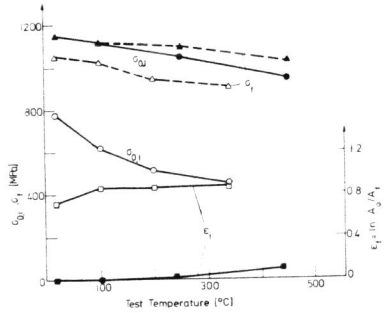

Figure 2 A: Tensile Properties versus Test Temperature.
Full Symbols: Ti-8Mo, Open Symbols: Ti-14Mo

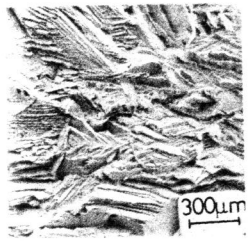

(a)

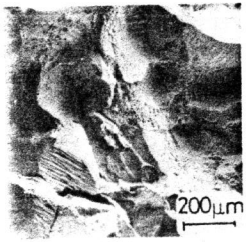

(b)

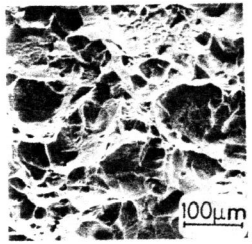

(c)

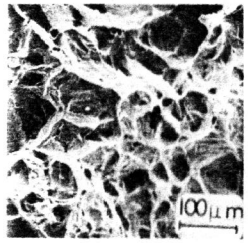

(d)

Figure 3 A: Fracture Topography as a Function of Test Temperature
(a) Ti-8Mo, RT; (b) Ti-8Mo, 450°C
(c) Ti-14Mo, RT; (d) Ti-14Mo, 350°C

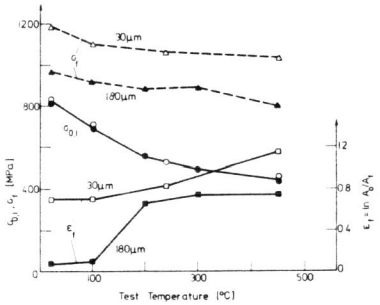

Figure 4 B: Tensile Properties versus Test Temperature Ti-14Mo

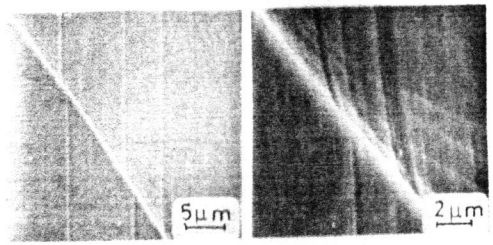

(a) (b)

Figure 5 B: Surface Sliding Along Grain Boundaries (PFZ). Ti-14Mo, Grain Size 180 µm.
(a) RT [4]; (b) 450°C

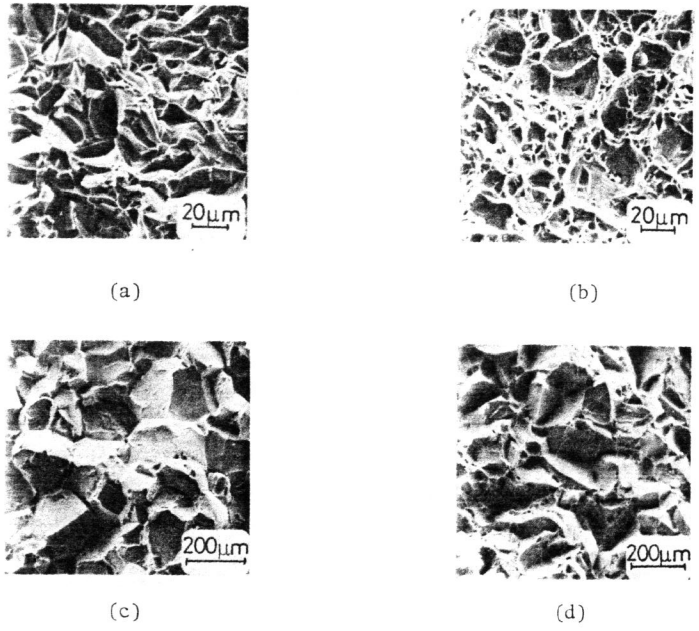

Figure 6 B: Fracture Topography as a Function of Test Temperature and Grain Size (GS). Ti-14Mo

(a) GS 30 µm, RT; (b) GS 30 µm, 450°C
(c) GS 180 µm, RT; (d) GS 180 µm, 450°C

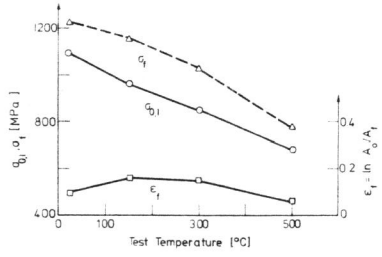

Figure 7 C: Tensile Properties versus Test Temperature Ti-8Mo

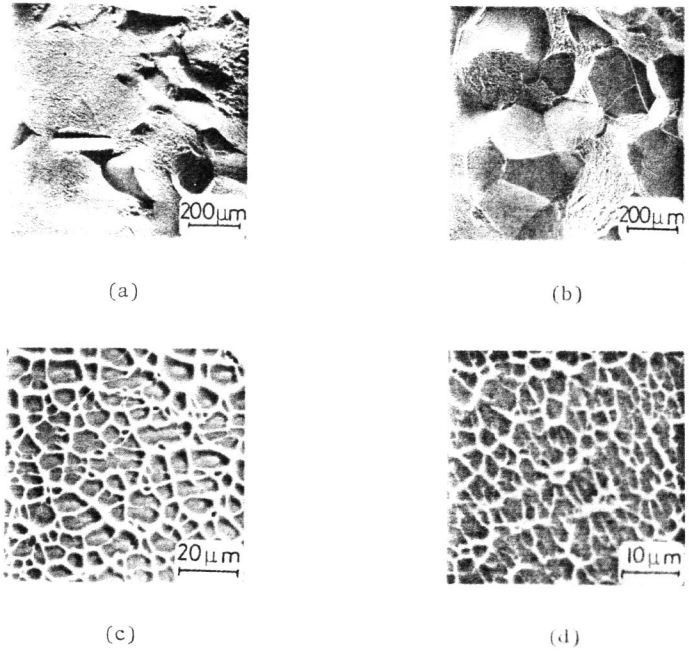

Figure 8 C: Fracture Topography as a Function of Test Temperature. Ti-8Mo

(a) RT; (b) 500°C; (c) RT; (d) 500°C